The GTCF Method for Exact Analysis of Multihop AF Relaying Systems

Norman C. Beaulieu, *Fellow, IEEE*, and Samy S. Soliman, *Student member, IEEE*
AITF/*i*CORE Wireless Communications Laboratory
University of Alberta, Edmonton, Alberta, T6G2V4 Canada
{beaulieu, soliman}@icoremail.ece.ualberta.ca

***Abstract*—A new transform method, the generalized transformed characteristic function (GTCF), gives an exact, integral solution for the probability density function of the end-to-end received signal-to-noise ratio (SNR) of multihop amplify-and-forward (AF) relaying systems. The results are precise for any number of hops and can accommodate any channel fading distribution. The theory provides the first exact theoretical solutions when the number of hops $N > 2$. Both cases of identically and non-identically distributed links are investigated. The case of dissimilar links, in which the link fadings follow different distributions, is also studied. The effect of the number of hops, N, on the performance metrics is studied.**

***Index Terms*—Average symbol error probability, cooperative networks, ergodic capacity, multihop relaying, outage probability.**

I. Introduction

Cooperative networks were recently proposed [1]–[8] as an efficient technique to mitigate wireless channel impairments as well as to significantly increase the system capacity and diversity gain in wireless networks. In addition, the cooperative networks concept is an efficient method for extending the coverage of wireless networks. The most common relaying techniques are amplify-and-forward (AF) and decode-and-forward (DF). Much research has focused on the performance of AF relaying systems because of lower complexity.

The outage probability and the average probability of error of dual-hop transmission over Rayleigh fading channels, and of multihop transmission over Nakagami-*m* fading channels were studied in [1] and [2], respectively. The authors presented an approximation for the end-to-end received signal-to-noise ratio (SNR) using the harmonic mean of independent random variables. Performance bounds on the outages and error probabilities of AF transmission over Nakagami-*m* fading channels were also obtained in [3], [4]. However, all the results in [3], [4] were based on the approximate harmonic mean expression for the end-to-end SNR. Bounds based on the harmonic mean approximation of the individual per hop instantaneous SNRs, are not tight for small-to-moderate values of SNR, and for Nakagami-*m* fading channels for large values of *m*. Moreover, increasing the number of hops may decrease the tightness of those bounds. For example, it was shown in [8] that the outage probability reported in [5] overestimates the real outage probability by 29.5 times. In [6], a new approximation was proposed in which the harmonic mean of the minimum of the first P hop SNRs and the minimum of the remaining hop SNRs is used to obtain new bounds. The new bounds were obtained for independent and non-identically distributed Rayleigh fading channels and for independent and identically distributed Nakagami-*m* fading channels for integer values of *m*. In [7], the authors presented a closed-form expression for the average bit error probability of AF fixed gain dual-hop relaying systems over Nakagami-*m* links for integer values of *m*. The expression involves a double-summation of complicated operands. The asymptotic average bit error probability, at large SNR, for arbitrary *m* was also evaluated.

Accurate performance analysis of cooperative diversity systems is important, as it enables the design of networks for maximum utility and performance and minimum cost. A previous work presented a new transform method for determining the exact end-to-end SNR distribution in AF cooperative relaying [8]. The generalized transformed characteristic function (GTCF) method [8] was used to obtain exact integral solutions for the ergodic capacity, outage probability and average symbol error probability of multihop AF relaying systems. The GTCF method is valid for any link fading distributions. In [8], only *identically* distributed Rayleigh and Nakagami-*m* fading links were studied while the cases of non-identically distributed channels and the case of Rician fading channels were not analyzed. The use of transform methods to solve difficult problems in a transform domain is a key approach in wireless communication theory (e.g. Fourier and Laplace transforms) and recent work [9], [10] has contributed new transform methods. This work presents a novel transform technique that can be used to solve heretofore difficult problems in cooperative wireless networks. In this follow-on work, we extend and continue the application of the GTCF method on more general link fading distributions. Examples will consider Rayleigh, Rician and Nakagami-*m* fading distributions. Both the independent and identically distributed (*i.i.d.*) case and the independent and non-identically distributed (*i.ni.d.*) case are examined. The case of dissimilar links, where the different links follow different fading distributions, is also investigated. A strength of the GTCF approach is that it can be used for any fading channel distribution with tractable computational effort. Closed-form expressions for the intermediate steps of the GTCF method are obtained to enhance the utility and reduce the computational complexity of the approach. We also study precisely the effect of the number of hops on the system performance in multihop relaying.

II. System Model

The multihop AF relaying system is shown in [8, Fig. 1]. The source node, R_0, and the destination node, R_N, communicate through $(N-1)$ intermediate relay nodes, $R_1, R_2, \cdots, R_{N-1}$. Each relay uses a variable gain to amplify the received signal before retransmitting it to the next node. The amplification factor, A_n, at the n^{th} relay node, R_n, is given by [1], [8] as $A_n = \sqrt{\frac{P_n}{P_{n-1}|\alpha_n|^2+N_{0n}}}$ where $P_n,\ n = 0, 1, \cdots, N-1$, is the transmitter power at the n^{th} node, and where $\alpha_n,\ n = 1, 2, \cdots, N$, and $N_{0n},\ n = 1, 2, \cdots, N$, are respectively the fading gain of the n^{th} link, and the noise power at the n^{th} node. We assume half-duplex operation and assume that orthogonal time slots are assigned to each of the transmitting nodes in order to avoid inter-signal-interference. The exact instantaneous end-to-end received SNR at the destination, γ_t, is given by [2, eq. (2)]

$$\gamma_t = \left[\prod_{n=1}^{N}\left(1+\frac{1}{\gamma_n}\right)-1\right]^{-1} \tag{1}$$

where $\gamma_n,\ n = 1, 2, \cdots, N$ represents the instantaneous received SNR over the n^{th} link defined as $\gamma_n = \frac{P_{n-1}}{N_{0n}}|\alpha_n|^2$.

The generalized transformed characteristic function (GTCF) method was developed to find the exact statistics of the instantaneous end-to-end SNR, γ_t. This allows finding exact solutions for the performance metrics such as the ergodic capacity, outage probability and the average symbol error probability. The GTCF approach was proposed and explained in detail in [8]. In the following, we summarize the procedure of the GTCF method. The main idea of the GTCF approach is that the expression in (1) can be rewritten as, $\left(1+\frac{1}{\gamma_t}\right) = \prod_{n=1}^{N}\left(1+\frac{1}{\gamma_n}\right)$. Then, taking the logarithm of both sides of this equation results in $Z_t = \sum_{n=1}^{N} Z_n$, where $Z_t = \ln\left(1+\frac{1}{\gamma_t}\right)$ and $Z_n = \ln\left(1+\frac{1}{\gamma_n}\right)$. With the assumption that $\gamma_n,\ n = 1, 2, \cdots, N$ are statistically independent, then the transformed random variables, Z_n, are statistically independent as well [11, p. 244]. The GTCF approach then proceeds as follows:

1. Find the PDF of the transformed random variables Z_n:
$$f_{z_n}(r) = \frac{e^r}{(e^r-1)^2} f_{\gamma_n}\left(\frac{1}{e^r-1}\right). \tag{2a}$$
2. Find the CHF of the transformed random variables Z_n:
$$\Phi_{Z_n}(\omega) = \int_0^\infty f_{z_n}(r) e^{j\omega r} dr. \tag{2b}$$
3. Find the CHF of the end-to-end transformed random variable Z_t:
$$\Phi_{Z_t}(\omega) = \prod_{n=1}^{N} \Phi_{Z_n}(\omega). \tag{2c}$$
4. Find the PDF of the end-to-end transformed random variable Z_t:
$$f_{z_t}(r) = \frac{1}{2\pi}\int_{-\infty}^{\infty} \Phi_{Z_t}(\omega) e^{-j\omega r} d\omega. \tag{2d}$$
5. Find the PDF of the end-to-end SNR γ_t:
$$f_{\gamma_t}(r) = \frac{1}{r(r+1)} f_{z_t}\left(\ln\left(1+\frac{1}{r}\right)\right). \tag{2e}$$

When the PDF of the instantaneous end-to-end SNR, γ_t, is available, different system performance metrics can be evaluated using [8, eqs. (13–15)].

III. The Characteristic Function of Z_n

As discussed in the previous section, the computation of the transformed characteristic function, $\Phi_{Z_n}(\omega)$, of the transformed random variable, Z_n, involves a single-fold integral as shown in (2b). In this section, we show that, for the common fading distributions, Rayleigh, Nakagami-*m* and Rician fadings, there exist closed-form expressions for the characteristic functions. To proceed, we substitute (2a) into (2b). Then, using the variable transformation, $x = \frac{1}{e^r-1}$, and after manipulation, (2b) is transformed into

$$\Phi_{Z_n}(\omega) = \int_0^\infty f_{\gamma_n}(x)\left(1+\frac{1}{x}\right)^{j\omega} dx. \tag{3}$$

For Nakagami-*m* fading links, $f_{\gamma_n}(x)$ is defined in [12]. Substituting the Nakagami-*m* fading distribution into (3) and transforming the resulting integral form we obtain

$$\Phi_{Z_n}(\omega) = C\,\Gamma(m-j\omega)\,U\left(m-j\omega,\ m+1,\ \frac{m}{\overline{\gamma}_n}\right) \tag{4}$$

where $C = \left(\frac{m}{\overline{\gamma}_n}\right)^m \frac{1}{\Gamma(m)}$ and $U(a,b,z)$ is the Tricomi confluent hypergeometric function defined in [13, eq. (13.2.5)]. Using a Kummer transformation [13, eq. (13.1.29)], namely $U(a,b,z) = z^{1-b}\,U(a-b+1, 2-b, z)$, a closed-form expression for the characteristic function, $\Phi_{Z_n}(\omega)$, in the case of Nakagami-*m* fading links, is obtained as

$$\Phi_{Z_n}(\omega) = \frac{1}{\Gamma(m)}\,\Gamma(m-j\omega)\,U\left(-j\omega,\ 1-m,\ \frac{m}{\overline{\gamma}_n}\right). \tag{5}$$

For Rician fading links, substituting the infinite series representation for the Bessel function $I_0(\cdot)$ [13, eq. (9.6.10)] into the PDF of the Rician fading distribution [12], and following the same procedure as before, the transformed characteristic function $\Phi_{Z_t}(\omega)$ can be written as

$$\Phi_{Z_n}(\omega) = \sum_{i=0}^{\infty} C_i\,\Gamma(i+1-j\omega)\,U(-j\omega,\ -i,\ \beta) \tag{6}$$

where $C_i = e^{-K}\frac{K^i}{(i!)^2}$, $\beta = \frac{1+K}{\overline{\gamma}}$ and K is the ratio of the power of the line-of-sight (LOS) component to the average power of the scattered component. Note that although the expression in (6) involves an infinite summation, it is found that the summands decay exponentially, or slightly faster, with increase of i, because Stirling's approximation specifies that $i!$ grows as $e^{i\ln i}$, and hence $\frac{1}{(i!)^2}$ decays as $e^{-2i\ln i}$, and hence, a truncated summation with a finite number of terms will reliably achieve a required accuracy.

By substituting (5) or (6) into (2c), we can obtain an expression for the characteristic function, $\Phi_{Z_t}(\omega)$, of the composite random variable Z_t in closed-form.

IV. Computational Considerations

A strength of the GTCF method is that in addition to providing exact results, which can be obtained for any general case of multihop AF systems with general fading distributions, it is computationally far less complex than other approaches that can give exact results. Previous exact methods, small in number, apply only for special cases of the AF systems.

In this section, we discuss the computational considerations and the ostensible complexity of the GTCF method. In some cases, the PDF of γ_t must be computed using (2e) and numerical integration of (2d). In this case, the GTCF method will require a 2-fold numerical integration. This is the case for Rayleigh, Rician and Nakagami-*m* link fading. In the case where no closed-form solutions are available for any of the integrals involved, but the link fadings are statistically identical or statistically identical to a scale factor, the GTCF method will require a 3-fold numerical integration. Note that the links can be statistically identical to a scale factor if the link SNRs follow the same distribution with the same fading parameters but they differ in the value of the average link SNRs, $\overline{\gamma}_n$. In the worst case where no closed-form solutions are available for any of the integrals involved and the links are not statistically identically distributed, the GTCF method will require a $(N+2)$-fold numerical integration, whether the links have dissimilar fading parameters or have different fading distributions. To see this, it can be shown that a performance metric can be expressed as

$$\int_0^\infty g_{\gamma_t}\left(\frac{1}{e^x-1}\right)\left(\frac{1}{2\pi}\int_{-\infty}^\infty \Phi_{Z_t}(\omega)e^{-j\omega x}d\omega\right)dx \qquad (7)$$

where $g_{\gamma_t}(\gamma_t)$ may represent the ergodic capacity for which $g_{\gamma_t}(\gamma_t)=\frac{1}{N}\log_2(1+\gamma_t)$ in [8, eq. (15)], or it may represent the average error probability for which $g_{\gamma_t}(\gamma_t)=Q(b\sqrt{a\gamma_t})$ in [8, eq. (13)]. Eq. (7) represents the composite integral expression for the GTCF method in the most general case. Table I shows the composite integral expressions required by the GTCF method, for different cases of complexity, cases (A), (B) and (D), and for exact evaluation using the distributions of the component link SNRs, case (C). We now explain cases (A), (B), (C) and (D) each in turn.

Case (A) occurs when a closed-form expression for $\Phi_{Z_n}(\omega)$ is known. For example, in the case of Nakagami-*m*, Rician or Rayleigh fading links, a closed-form expression for $\Phi_{Z_t}(\omega)$ can be obtained by substituting the suitable expressions for $\Phi_{Z_n}(\omega)$ into (2c). Substituting the obtained expression for $\Phi_{Z_t}(\omega)$ into (7) results in the 2-fold integral expression (A) in Table I. In the worst case, when the double-integral expression (7) can not be evaluated in closed-form, it can be numerically evaluated using available software packages such as MATLAB and MATHEMATICA. Note that numerical calculation of a 2-fold integral is widely practised in the literature.

Case (B) occurs when no closed-form expression for $\Phi_{Z_n}(\omega)$ is known, but the link fadings are statistically identical or statistically identical to a scale factor. In this case, the characteristic functions, $\Phi_{Z_n}(\omega)$, are compressed, or expanded, versions of each other. In these cases, the integral definition in (2b) will be used and the performance metrics are represented by (B) in Table I. Evaluation of this representation involves a 3-fold numerical integral because the numerical calculation of the innermost integral in (B) is done only once, resulting in a computational complexity of 3 nested numerical integrals.

TABLE I
Representations of the integration complexity of the different cases using the GTCF method

Case	Representation
(A) *(2)-* fold	$\int_0^\infty g_{\gamma_t}\left(\frac{1}{e^x-1}\right)\left(\frac{1}{2\pi}\int_{-\infty}^\infty \prod_{n=1}^N \left[\Phi_{Z_n}(\omega)\right]e^{-j\omega x}d\omega\right)dx$
(B) *(3)-* fold	$\int_0^\infty g_{\gamma_t}\left(\frac{1}{e^x-1}\right) \times\left(\frac{1}{2\pi}\int_{-\infty}^\infty \left[\int_0^\infty f_{z_n}(\sigma)e^{j\omega\sigma}d\sigma\right]^N e^{-j\omega x}d\omega\right)dx$
(C) *(N)-* fold	$\int_{r_N=0}^\infty\int_{r_{N-1}=0}^\infty\cdots\int_{r_1=0}^\infty g_{\gamma_t}\left(\left[\prod_{n=1}^N\left(1+\frac{1}{r_n}\right)-1\right]^{-1}\right) \times f_{\gamma_N}(r_N)f_{\gamma_{N-1}}(r_{N-1})\cdots f_{\gamma_1}(r_1)\,dr_1\cdots dr_{N-1}dr_N$
(D) *(N+2)-* fold	$\int_0^\infty g_{\gamma_t}\left(\frac{1}{e^x-1}\right) \times\left(\frac{1}{2\pi}\int_{-\infty}^\infty \prod_{n=1}^N\left[\int_0^\infty f_{z_n}(\sigma)e^{j\omega\sigma}d\sigma\right]e^{-j\omega x}d\omega\right)dx$

Case (C) represents the integration complexity of exact evaluation using the PDFs of the component link SNRs. The representation (C) in Table I involves a N-fold integral. This N-fold integral can not be simplified even when the links are identical, because of the presence of the complicated, inseparable function, $g_{\gamma_t}(\gamma_t)$, where γ_t is defined in (1). This clarifies the computational advantage of using the GTCF method in cases (A) and (B), especially for large numbers of links, N.

Finally, case (D) occurs when no closed-form expression for $\Phi_{Z_n}(\omega)$ is known and the individual links have different fading distributions or similar fading distributions with different fading parameters. In this case, calculation of the performance metrics using the GTCF method requires a $(N+2)$-fold numerical integration as shown by (D) in Table I.

V. Numerical Examples

In this section, we use the GTCF method to investigate the performance of multihop AF relaying systems. Multihop systems with *i.i.d.*, *i.ni.d.* and dissimilar links are considered. We assume an uniform power allocation policy, that is the total available power, *P*, is evenly allocated to the source and the relays. Without loss of generality, we assume equal noise powers, N_0, at all the nodes. The nodes are assumed to be located at equal distances from each other, and normalized distances are assumed, i.e. $d_{hop}=\frac{1}{N}$, so according to the Friss propagation model [14], the average SNR over any link is given as $\overline{\gamma}=N^{\delta-1}\frac{P}{N_0}$ where δ is the path loss component, taken equal to 3 in the following examples and

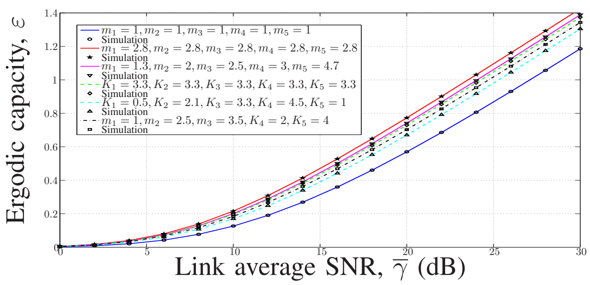

Fig. 1. The ergodic capacity for a five-hop ($N = 5$) AF relaying systems.

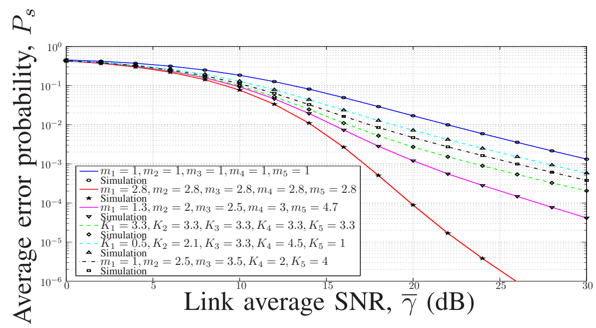

Fig. 2. The average error probability for a five-hop ($N = 5$) AF relaying systems with BPSK modulation.

binary phase shift keying (BPSK) modulation is assumed. Note that we make these simplifying assumptions in the examples for convenience; they are not required by the analysis.

The first set of examples is intended to confirm the accuracy and versatility of the GTCF approach. The GTCF method is used to obtain the average error probability, outage probability and the ergodic capacity for a five-hop ($N = 5$) AF system with *i.i.d.* Rayleigh, Nakagami-*m* ($m = 2.8$) and Rician ($K = 3.3$) fading links. The same system performance metrics are shown for *i.ni.d.* Nakagami-*m* fading links, ($m_1 = 1.3, m_2 = 2, m_3 = 2.5, m_4 = 3, m_5 = 4.7$) and *i.ni.d.* Rician fading links, ($K_1 = 0.5, K_2 = 2.1, K_3 = 3.3, K_4 = 4.5, K_5 = 1$). A hybrid case, where the first link fading is Rayleigh distributed, the second and the third link fadings are Nakagami-*m* distributed, while the fourth and the fifth link fadings are Rician distributed, ($m_1 = 1, m_2 = 2.5, m_3 = 3.5, K_4 = 2, K_5 = 4$), is also investigated. As expected from the analysis, Figs. 1, 2 and 3 show precise agreement between the results obtained from the GTCF method and simulation results at all values of $\overline{\gamma}$ for the different performance measures.

The figures show some interesting aspects of the performance measures and their relationship to the type of fading. Fig. 1 shows that the ergodic capacity is better for the less severely faded Nakagami-*m* and Rician fading channels than the Rayleigh channels. For example, the ergodic capacity at $\overline{\gamma} = 26\,dB$ is 0.93 in the case of Rayleigh fading links, while it is 1.11 and 1.16 for identically distributed Rician ($K = 3.3$) and Nakagami-*m* ($m = 2.8$) links, respectively. However, more dramatic differences in performance are seen in the average error probability in Fig. 2 and the outage probability in Fig. 3. It is observed that although the Rician links outperform the Rayleigh links, the limiting slopes of the average error probability curves, in the case of Rician fading links, are the same as the slope of the average error probability in the case of Rayleigh fading links. A similar behaviour is observed in the outage probability curves. In contrast, the behaviour of the Nakagami-*m* links is markedly different. The limiting slopes of the average error probability curves in Fig. 2 and the limiting slope of the outage probability curves in Fig. 3 are greater than those for the Rician and Rayleigh curves and the limiting slopes change with variation of the fading parameters, m_n. The dependence of the limiting slopes of the performance curves on the fading parameter m dictates that the Nakagami-*m* model will always exhibit better performance than the Rician model,

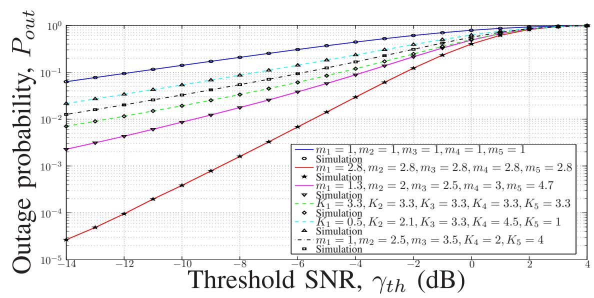

Fig. 3. Outage probability for a five-hop ($N = 5$) AF relaying system at $\overline{\gamma} = 10\,dB$.

for sufficiently large SNR for all values of $m > 1$, regardless of the value of the Rician parameter K. For example, an outage probability of 10^{-2} occurs at $\gamma_{th} = -12.6\,dB$ in the case of Rician fading links with $K = 3.3$, while it occurs at $\gamma_{th} = -5.5\,dB$ in the case of Nakagami-*m* fading links with $m = 2.8$. The results show also that even in the case when one of the links has a large LOS factor, e.g. $K_4 = 4.5$ in the case of *i.ni.d.* Rician fading links, the performance of Nakagami-*m* links is still superior for sufficiently large SNR. For example, an average error probability of 10^{-3} occurs at $\overline{\gamma} = 27.7\,dB$ for the case of *i.ni.d.* Rician fading links, while it occurs at $\overline{\gamma} = 17.1\,dB$ for the case of *i.i.d.* Nakagami-*m* fading links. It is observed also that the system performance is limited by the fading parameters of the "weakest" link in the multihop path.

The next example emphasizes the previous observations and shows further interesting observations. Fig. 4 shows the average error probability for different cases of five-hop AF relaying systems over Nakagami-*m* fading links. The first two cases represent *i.i.d.* Rayleigh and Nakagami-*m* ($m = 2$) links. The other three cases represent *i.ni.d.* Nakagami-*m* links with different values of the fading parameters m_n as shown in the legend of the figure. In case (3), $\min\{m_n\} = 1$ while in cases (4) and (5), $\min\{m_n\} = 1.5$ and 2, respectively. It is observed that the limiting slopes of the average error probability curves is dependent only on the minimum value of the fading parameters, $\min\{m_n\}$. It is shown in Fig. 4 that the limiting slope of case (1), where ($m_n = 1$), is the same as the limiting slope of case (3), where $\min\{m_n\} = 1$. The same observation is true for cases (2) and (5). Note that the dependence of the limiting slope of the average error

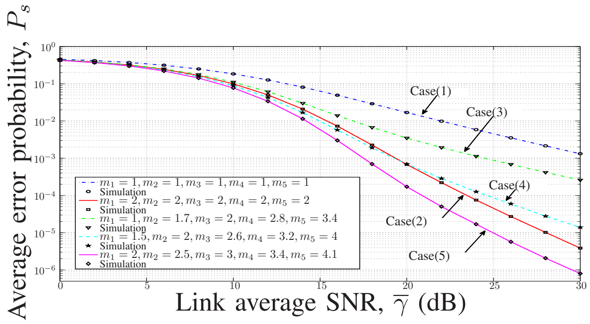

Fig. 4. The average error probability for a five-hop ($N = 5$) AF relaying systems with BPSK modulation. Different cases of Nakagami-*m* links are assumed.

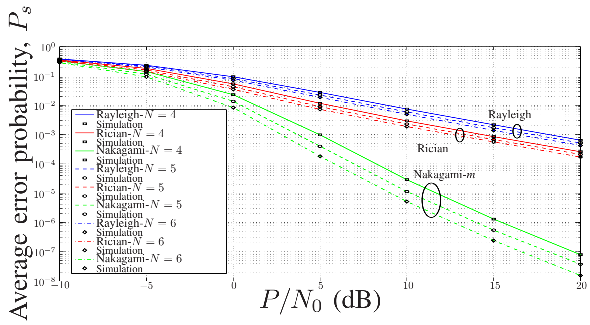

Fig. 5. The average error probability for a multihop ($N = 4, 5$ and 6) AF relaying systems with BPSK modulation.

probability curve on the value of the smallest fading parameter, $\min\{m_n\}$, is not affected by the placement of the link which attains this smallest value of the fading parameters. This can be seen from (1) which shows that the instantaneous end-to-end SNR, γ_t, is symmetric with respect to all the individual link SNRs, γ_n. On the other hand as expected, the larger the values of the fading parameters, other than the smallest one, the better the performance of the system. For example, at $\overline{\gamma} = 28\ dB$, the average error probability for case (2) is 1.0×10^{-5}, while it is 2.1×10^{-6} for case (5) where $m_1 = 2$, $m_2 = 2.5$, $m_3 = 3$, $m_4 = 3.4$, $m_5 = 4.1$.

The next examples study the effect of increasing the number of hops on the different performance metrics. The average error probability is shown in Fig. 5 for multihop AF relaying systems with $N = 4, 5$ and 6. Rayleigh, *i.i.d.* Nakagami-*m* ($m = 2.5$) and *i.i.d.* Rician ($K = 2$) fading channels are considered in the examples. The ergodic capacity is also shown in Fig. 6 for the *i.i.d.* Nakagami-*m* and Rician links. The first observation is that the limiting slope of the average error probability curves, for all fading distribution cases, is independent of the number of hops, *N*. Note that the system model assumes that the data signal is received at the destination through only the multihop relay path. On the other hand, there is an effective SNR gain achieved by using more intermediate relays. To achieve an average error probability of 10^{-5} over the Nakagami-*m* links, a five-hop system requires $1.50\ dB$ less total power than that required by a four-hop system, while a six-hop system requires $2.64\ dB$ less total power.

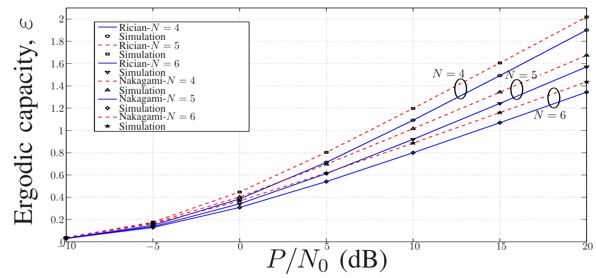

Fig. 6. The ergodic capacity for a multihop ($N = 4, 5$ and 6) AF relaying systems.

Another observation concerning the ergodic capacity can be drawn from Fig. 6. It can be noticed that with increasing the number of hops, N, the ergodic capacity, ε, decreases. For example, for the Rician fading case at $P/N_0 = 15\ dB$, the ergodic capacities for $N = 4, 5$ and 6 are $1.492, 1.242$ and 1.069. The decrease in the ergodic capacity is to be expected. Since the relaying is time division multiplexed on orthogonal channels, the time-bandwidth resources consumed to send the message end-to-end increases with the number of relaying transmissions and the capacity per link decreases when fixed bandwidth transmission is employed.

REFERENCES

[1] M. O. Hasna and M. S. Alouini, "End-to-end performance of transmission systems with relays over Rayleigh-fading channels," *IEEE Trans. Wireless Commun.*, vol. 2, no. 6, pp. 1126–1131, Nov. 2003.

[2] ——, "Outage probability of multihop transmission over Nakagami fading channels," *IEEE Commun. Lett.*, vol. 7, no. 5, pp. 216–218, May 2003.

[3] G. K. Karagiannidis, T. A. Tsiftsis, and R. K. Mallik, "Bounds for multihop relayed communications in Nakagami-*m* fading," *IEEE Trans. Commun.*, vol. 54, no. 1, pp. 18–22, Jan. 2006.

[4] G. Farhadi and N. C. Beaulieu, "A general framework for symbol error probability analysis of wireless systems and its application in amplify-and-forward multihop relaying," *IEEE Trans. Veh. Technol.*, vol. 59, no. 3, pp. 1505–1510, Mar. 2010.

[5] C. Tellambura, M. Soysa, and D. Senaratne, "Performance analysis of wireless systems from the MGF of the reciprocal of the signal-to-noise ratio," *IEEE Commun. Lett.*, vol. 15, no. 1, pp. 55–57, Jan. 2011.

[6] G. Amarasuriya, C. Tellambura, and M. Ardakani, "Performance bounds for AF multi-hop relaying over Nakagami fading," in *IEEE Wireless Commun. and Networking Conf.*, Sydney, Australia, Apr. 2010, pp. 1–6.

[7] H. A. Suraweera and G. K. Karagiannidis, "Closed-form error analysis of the non-identical Nakagami-*m* relay fading channel," *IEEE Commun. Lett.*, vol. 12, no. 4, pp. 259–261, Apr. 2008.

[8] N. C. Beaulieu and S. S. Soliman, "Exact analytical solution for end-to-end SNR of multihop AF relaying systems," in *GLOBECOM Workshops (GC Wkshps), 2011 IEEE*, Houston, Tx, Dec. 2011, pp. 580–585.

[9] A. Conti, W. Gifford, M. Win, and M. Chiani, "Optimized simple bounds for diversity systems," *IEEE Trans. Commun.*, vol. 57, no. 9, pp. 2674–2685, Sep. 2009.

[10] W. Gifford, M. Win, and M. Chiani, "Antenna subset diversity with non-ideal channel estimation," *IEEE Trans. Wireless Commun.*, vol. 7, no. 5, pp. 1527–1539, May 2008.

[11] A. Papoulis and S. U. Pillai, *Probability, Random Variables and Stochastic Processes*, 4th ed. Boston: McGraw-Hill, 2002.

[12] M. K. Simon and M.-S. Alouini, *Digital Communication over Fading Channels*, 2nd ed. New York: Wiley, 2005.

[13] M. Abramowitz and I. A. Stegun, *Handbook of Mathematical Functions with Formulas, Graphs, and Mathematical Tables*, 9th ed. New York: Dover, 1972.

[14] T. S. Rappaport, *Wireless Communications: Principles and Practice*. Englewood Cliffs: Prentice-Hall, 1996.